

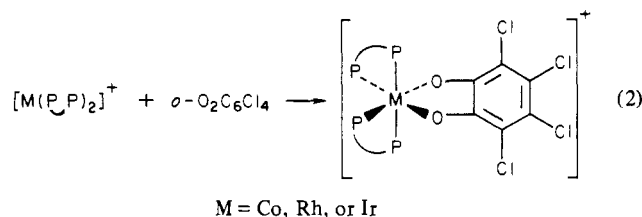
Table I. Enthalpy Data for the Reaction between $[M(\text{Ph}_2\text{PCH}=\text{CHPh}_2)_2]\text{BF}_4$ and $\text{O}_2\text{C}_6\text{Cl}_4$ in 1,2-Dichloroethane at 25 °C

M	$-\Delta H, ^\circ\text{kJ/mol}$
Co	196 ± 11
Rh	144 ± 9
Ir	179 ± 8

^a Error limits are 1 standard deviation of the mean of at least 12 determinations.

temperatures in order to eliminate carbon monoxide from the initial reaction product, which is $[\text{Ir}(\text{CO})(\text{Ph}_2\text{PCH}=\text{CHPh}_2)_2]^+$.⁹ The analogous rhodium complex is readily obtained from $[\text{RhCl}(1,5\text{-C}_8\text{H}_{12})_2]$ in a similar way.

When a solution of $[M(\text{Ph}_2\text{PCH}=\text{CHPh}_2)_2]\text{BF}_4$ was tritrated with a solution of tetrachloro-*o*-benzoquinone, heat was liberated and the end point reached with equimolar amounts of the reactants. Further addition of the titrant produced no heat change, showing 1:1 stoichiometry. A similar result was obtained in the reverse titration. The stoichiometry was further confirmed by isolation of $[M(\text{O}_2\text{C}_6\text{Cl}_4)(\text{Ph}_2\text{PCH}=\text{CHPh}_2)_2]\text{BF}_4$ from solutions of rather higher concentrations than those used in calorimetric titrations. The reaction shown in eq 2 is clean and quantitative.



The tendency of d^8 complexes to undergo oxidative addition increases in going from the second to the third transition series in a given group of the periodic table.⁴ The relative position of the metal in the first transition series is often not known because the appropriate complexes are not available. Quantitative comparison of their reactivity toward various addends is only possible with complexes having a similar ligand environment.^{3,5}

The complexes $[M(\text{Ph}_2\text{PCH}=\text{CHPh}_2)_2]^+$ have a planar structure¹⁴ like $[M(\text{Ph}_2\text{PCH}_2\text{CH}_2\text{PPh}_2)_2]^+$ ¹⁵ and many other d^8 complexes. The higher reactivity of the iridium complex over the rhodium analogue is suggested by the fact that $[\text{Ir}(\text{Ph}_2\text{PCH}_2\text{CH}_2\text{PPh}_2)_2]^+$ readily adds hydrogen to give six-coordinate Ir(III) but the corresponding Rh complex does not.^{14,16} The crystal structure of the dioxygen adducts $[M(\text{O}_2)(\text{Ph}_2\text{PCH}_2\text{CH}_2\text{PPh}_2)_2]\text{PF}_6$ ¹⁷ (M = Rh, Ir) shows that the Ir-O bonds are longer compared to the Rh-O bonds. Vaska has suggested on the basis of qualitative evidence that the stability of adducts is $\text{Co} > \text{Ir} > \text{Rh}$.⁹

Table I shows the enthalpy data obtained from calorimetric titrations. Comparison of data shows that $\Delta H_{\text{Rh}} \approx 0.8(\Delta H_{\text{Ir}})$, which agrees well with the ΔH ratio for the reaction of $\text{MX}(\text{CO})\text{L}_2$ (M = Rh, Ir) with $\text{O}_2\text{C}_6\text{Cl}_4$ in benzene.¹⁸ It is also observed qualitatively here that the sequence of reactivity (kinetic) of the three metal complexes for oxidative addition is $\text{Co} > \text{Ir} > \text{Rh}$. Since the reactions are virtually quantitative having $K \geq 10^5$ L/mol, it is not possible to compare quantitatively the adduct stabilities, which are very likely to be consistent with the order suggested by Vaska⁹ for formation

Table II. Physical Properties of the Complexes $[M(\text{O}_2\text{C}_6\text{Cl}_4)(\text{Ph}_2\text{PCH}=\text{CHPh}_2)_2]\text{BF}_4$

M	color	mp, °C	λ_{max} , nm (ϵ)	IR for the three complexes, ^a cm^{-1}
Co	green	214-217 dec	337 (26 000)	} 1260 (m), ~1060 (s), 970 (m), 810 (m)
Rh	purple	365-368 dec	544 (1205)	
Ir	orange	340-342 dec	437 (1222)	

^a Abbreviations: m, medium; s, strong.

of $[M(\text{O}_2)(\text{Ph}_2\text{PCH}=\text{CHPh}_2)_2]^+$ in chlorobenzene. The enthalpy data when compared to data¹⁷ for $\text{MX}(\text{CO})(\text{PPh}_3)_2$ indicate that the chelate complexes form stronger bonds with $\text{O}_2\text{C}_6\text{Cl}_4$ and may thus be considered as stronger bases. This coincides with the fact that H_2 and O_2 addition to $[\text{Ir}(\text{Ph}_2\text{PCH}_2\text{CH}_2\text{PPh}_2)_2]^+$ is irreversible while these molecules are readily removed from *trans*- $[\text{IrCl}(\text{CO})(\text{PPh}_3)_2]$ by heating.⁹ The higher enthalpy change for reaction of the cobalt complex in comparison to those of rhodium and iridium and the apparent greater reactivity toward dioxygen may arise from the relative instability of cobalt(I) in a square-planar environment.

Some of the physical properties of the oxidative-addition products are given in Table II. The complexes have high thermal stability. The intense absorption in the visible region by the cobalt complex and comparatively less intense absorptions by rhodium and iridium complexes are presumably due to charge-transfer transitions. The IR spectra of all three complexes show absorptions at the same wavelengths, indicating that the addition complexes have the same structures. Attempts to obtain satisfactory ¹H NMR spectra were frustrated by the low solubility of the complexes.

Acknowledgment. We gratefully acknowledge the support of the Robert A. Welch Foundation and the University of Texas at Arlington Organized Research Fund for support of this work. A loan of iridium chloride from Engelhard, Inc., is also appreciated.

Registry No. $[\text{Co}(\text{Ph}_2\text{PCH}=\text{CHPh}_2)_2]\text{BF}_4$, 80243-31-8; $[\text{Co}(\text{O}_2\text{C}_6\text{Cl}_4)(\text{Ph}_2\text{PCH}=\text{CHPh}_2)_2]\text{BF}_4$, 80243-33-0; $[\text{Rh}(\text{Ph}_2\text{PCH}=\text{CHPh}_2)_2]\text{BF}_4$, 54293-56-0; $[\text{Rh}(\text{O}_2\text{C}_6\text{Cl}_4)(\text{Ph}_2\text{PCH}=\text{CHPh}_2)_2]\text{BF}_4$, 80262-56-2; $[\text{Ir}(\text{Ph}_2\text{PCH}=\text{CHPh}_2)_2]\text{BF}_4$, 80243-34-1; $[\text{Ir}(\text{O}_2\text{C}_6\text{Cl}_4)(\text{Ph}_2\text{PCH}=\text{CHPh}_2)_2]\text{BF}_4$, 80243-36-3; $\text{O}_2\text{C}_6\text{Cl}_4$, 2435-53-2; $\text{CoCl}(\text{PPh}_3)_3$, 26305-75-9; $[\text{RhCl}(\text{COD})]_2$, 12092-47-6; $\text{IrClN}_2(\text{PPh}_3)_2$, 15695-36-0.

Contribution from the Institute of Scientific and Industrial Research, Osaka University, Suita, Osaka 565, Japan

Synthesis and Magnetic Properties of $(\text{Mn}_{1-x}\text{Cr}_x)_3\text{B}_4$ and $(\text{Mn}_{1-x}\text{Mo}_x)_3\text{B}_4$

T. Ishii, M. Shimada,* and M. Koizumi

Received August 11, 1981

Mn_3B_4 has the orthorhombic (D_{7h}) Ta_3B_4 -type structure and is antiferromagnetic with a Néel temperature of 392 K. But the temperature dependence of magnetic susceptibility of Mn_3B_4 shows a second magnetic ordering at 226 K.¹ On the basis of the magnetic structure determined by neutron diffraction, Neov² reported that below 226 K the Mn4(g) atoms were magnetically ordered and the collinear antiferromagnetic structure was deformed to a spiral structure, and that at 4.2 K the collinear antiferromagnetic structure was recovered

- (14) Vaska, L.; Catone, D. L. *J. Am. Chem. Soc.* **1966**, *88*, 5324.
 (15) Hall, M. C.; Kilbourn, B. T.; Taylor, K. A. *J. Chem. Soc. A* **1970**, 2539.
 (16) Taylor, K. A. *Adv. Chem. Ser.* **1968**, No. 70, 195.
 (17) McGinney, J. A.; Payne, N. C.; Ibers, J. A. *J. Am. Chem. Soc.* **1969**, *91*, 6301.
 (18) Burke, N. E.; Singhal, A.; Hintz, M. J.; Ley, J. A.; Hui, H.; Smith, L. R.; Blake, D. M. *J. Am. Chem. Soc.* **1979**, *101*, 74.

- (1) Yanase, A. *J. Phys. Soc. Jpn.* **1965**, *20*, 1596.
 (2) Neov, S.; Legrand, E. *Phys. Status Solidi B* **1972**, *49*, 589.

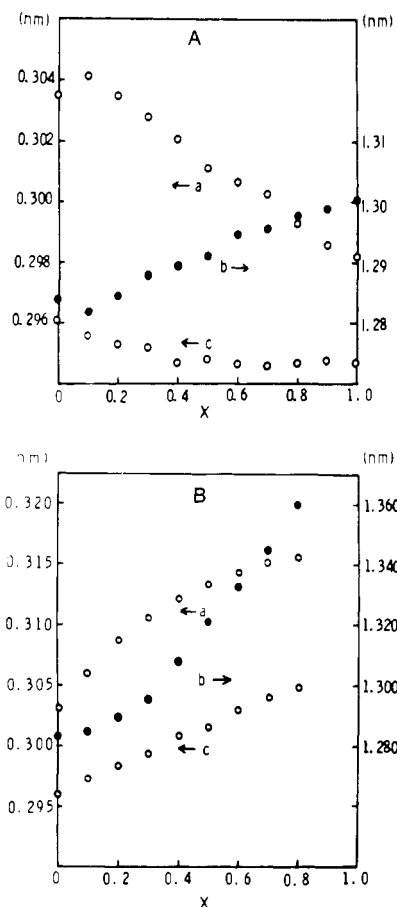


Figure 1. Lattice constants vs. composition in the systems (A) $(\text{Mn}_{1-x}\text{Cr}_x)_3\text{B}_4$ and (B) $(\text{Mn}_{1-x}\text{Mo}_x)_3\text{B}_4$.

again. The saturated magnetic moments at 4.2 K are $2.92 \mu_B$ for the Mn2(c) atoms and $0.44 \mu_B$ for the Mn4(g) atoms.

Since Mn_3B_4 exhibits layered type strong ferromagnetic coupling in the *ac* plane and weak antiferromagnetic coupling between layers, the antiferromagnetic compound Mn_3B_4 has a highly positive paramagnetic Curie temperature of 543 K.

Further studies on the magnetic properties of this compound have been carried out by substituting manganese atoms with other transition elements. Tawara reported that the magnetic properties changed drastically from antiferromagnetic to ferromagnetic due to the coexistence of a ferromagnetic compound, Mn_2CrB_4 or Mn_2MoB_4 , in the system $(\text{Mn}_{1-x}\text{Cr}_x)_3\text{B}_4$ and $(\text{Mn}_{1-x}\text{Mo}_x)_3\text{B}_4$.^{3,4} According to his reports, the solid solution ranges in both systems were quite narrow, because temperature conditions of synthesis were limited to below 1100 °C due to use of an evacuated quartz tube.

In the present investigation a high-pressure technique was used for the preparation of high-temperature materials. By this method a closed system was available under high-temperature conditions of 2000 °C for solid-state reactions.

With use of the above technique, an attempt was made to synthesize the solid solution $(\text{Mn}_{1-x}\text{Cr}_x)_3\text{B}_4$ ($0 \leq x \leq 1$) and $(\text{Mn}_{1-x}\text{Mo}_x)_3\text{B}_4$ ($0 \leq x \leq 0.8$) to examine the effect of replacement of Mn with Cr and Mo on the magnetic properties.

Experimental Section

Starting materials of $(\text{Mn}_{1-x}\text{Cr}_x)_3\text{B}_4$ and $(\text{Mn}_{1-x}\text{Mo}_x)_3\text{B}_4$ were prepared by mixing manganese (99.9%), chromium (99.9%), molybdenum (99.9%), and boron (99.9%) powders in desired ratios. The powders were put into a cylindrical BN capsule, which was placed

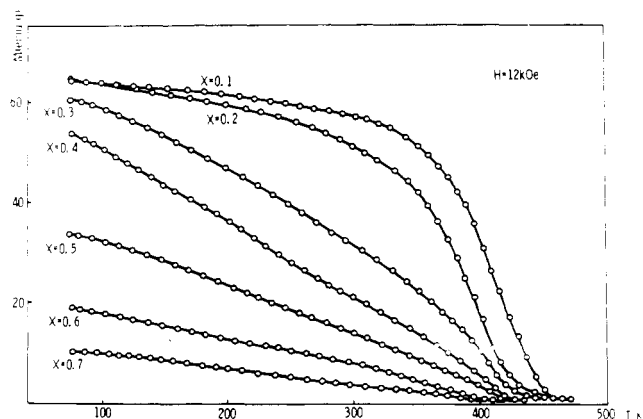


Figure 2. Temperature dependence of the magnetization of $(\text{Mn}_{1-x}\text{Cr}_x)_3\text{B}_4$.

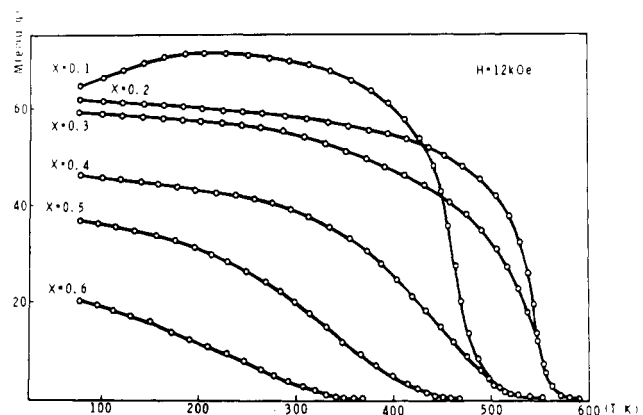


Figure 3. Temperature dependence of the magnetization of $(\text{Mn}_{1-x}\text{Mo}_x)_3\text{B}_4$.

in a carbon heater. This assemblage was put into a pyrophyllite cube. The cube was subjected to high-temperature-high-pressure conditions with use of a cubic anvil type apparatus.

The magnitude of pressure generated inside the cell was calibrated on the basis of the electrical transition of Bi (2.55 GPa) and Ba (5.5 GPa). The temperature of the sample was measured by a Pt—Pt—13% Rh thermocouple in the center of the cube. The reaction was carried out at 3.0 GPa and 1800–1900 °C for 10–30 min. The products were identified by X-ray powder diffraction. Lattice parameters were determined by a least-squares method from the powder patterns. Silicon was used as an internal standard. Magnetic measurements were performed with a magnetic torsion balance in the temperature range of 4.2–900 K in a field of 12 kOe.

Results and Discussion

X-ray powder diffraction patterns of all samples of $(\text{Mn}_{1-x}\text{Cr}_x)_3\text{B}_4$ ($0 \leq x \leq 1$) and $(\text{Mn}_{1-x}\text{Mo}_x)_3\text{B}_4$ ($0 \leq x \leq 0.8$) synthesized under high-pressure-high-temperature conditions were completely indexed as the Ta_3B_4 type structure. The relation between composition and lattice parameters of $(\text{Mn}_{1-x}\text{Cr}_x)_3\text{B}_4$ and $(\text{Mn}_{1-x}\text{Mo}_x)_3\text{B}_4$ is shown in Figure 1. The lattice parameters of Mn_3B_4 synthesized in the present experiments were in good agreement with those reported by Kiessling,⁵ but those of Cr_3B_4 were a little smaller than those of published data.⁶

As seen in Figure 1, the compositional dependence of the lattice constants of both the *a* and *b* axes in $(\text{Mn}_{1-x}\text{Cr}_x)_3\text{B}_4$ did not change monotonously but showed a cuplike variation. The *a* axis had a maximum and the *b* axis had a minimum at $x = 0.1$. Similar changes of both lattice parameters for *a* and *b* axes were observed in the system of $(\text{Mn}_{1-x}\text{Mo}_x)_3\text{B}_4$. In

(3) Tawara, Y.; Iga, A.; Yanase, A. *J. Phys. Soc. Jpn.* **1966**, *21*, 476.
(4) Tawara, Y.; Iga, A. *J. Phys. Soc. Jpn.* **1968**, *24*, 28.

(5) Kiessling, R. *Acta Chem. Scand.* **1950**, *4*, 146.
(6) Kiessling, R. *Acta Chem. Scand.* **1950**, *4*, 160.

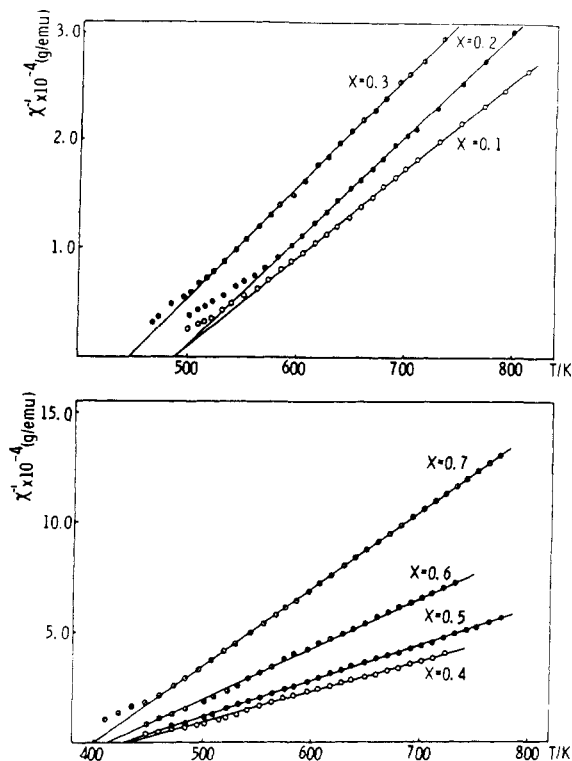


Figure 4. Temperature dependence of the reciprocal susceptibility of $(\text{Mn}_{1-x}\text{Cr}_x)_3\text{B}_4$.

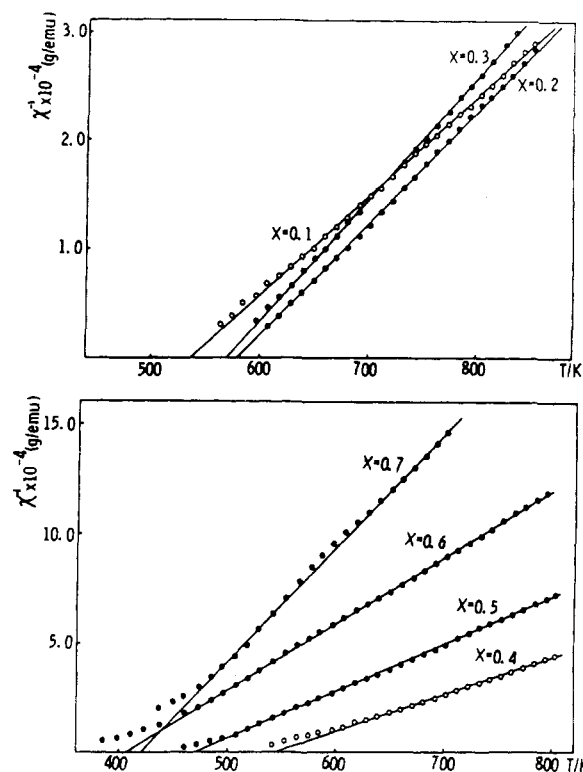


Figure 5. Temperature dependence of the reciprocal susceptibility of $(\text{Mn}_{1-x}\text{Mo}_x)_3\text{B}_4$.

both systems, however, the c axis changed monotonously. The curious change of lattice parameters vs. composition is due to the magnetic contribution, because the magnetic properties of the system $(\text{Mn}_{1-x}\text{Cr}_x)_3\text{B}_4$ in the range of $0.1 \leq x \leq 0.7$ and the system $(\text{Mn}_{1-x}\text{Mo}_x)_3\text{B}_4$ in the range of $0.1 \leq x \leq 0.6$ are both ferromagnetic above room temperature.

The temperature dependences of magnetization of the systems $(\text{Mn}_{1-x}\text{Cr}_x)_3\text{B}_4$ and $(\text{Mn}_{1-x}\text{Mo}_x)_3\text{B}_4$ are shown in Figures 2 and 3.

The magnetization curve of the sample with $x = 0.1$ in the system $(\text{Mn}_{1-x}\text{Mo}_x)_3\text{B}_4$ was quite curious and was similar in form to that expected for a ferromagnetic substance of Néel's type P.⁷ Since the asymptotic Curie temperature had a large positive value, however, it is likely that this change of magnetization is attributable to the canted spin structure.

The temperature dependences of reciprocal susceptibility of the ferromagnetic samples of $(\text{Mn}_{1-x}\text{Cr}_x)_3\text{B}_4$ and $(\text{Mn}_{1-x}\text{Mo}_x)_3\text{B}_4$ are shown in Figures 4 and 5. All samples obeyed the Curie-Weiss law in the paramagnetic region. The fact that the paramagnetic Curie temperatures of all samples were positive indicates that the predominant superexchange interactions were ferromagnetic.

The paramagnetic moment per molecule calculated from the Curie constant is shown in Figure 6 as a function of the mole fraction x . Since Cr_3B_4 exhibited no magnetic ordering state even down to 4.2 K, it is assumed that it probably does not have a localized magnetic moment. The paramagnetic moments of both solid solutions were calculated with the assumption that Mn_3B_4 had a magnetic moment of $4.42 \mu_B/\text{mol}$ and Cr and Mo had no localized magnetic moment. These calculated values are shown as the dotted line in Figure 6. As seen in Figure 6, the experimental values were in good agreement with the calculated ones, and it was considered that Cr and Mo were substituted into Mn_3B_4 without a localized magnetic moment.

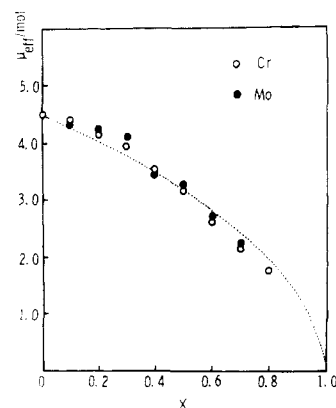


Figure 6. Paramagnetic moment of $(\text{Mn}_{1-x}\text{M}_x)_3\text{B}_4$ ($\text{M} = \text{Cr}, \text{Mo}$).

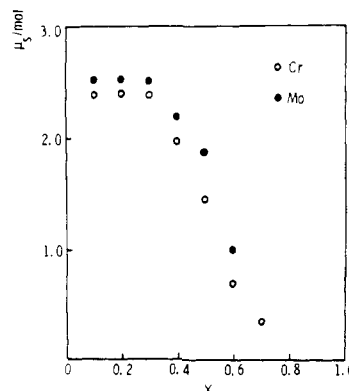


Figure 7. Ferromagnetic moment of $(\text{Mn}_{1-x}\text{M}_x)_3\text{B}_4$ ($\text{M} = \text{Cr}, \text{Mo}$).

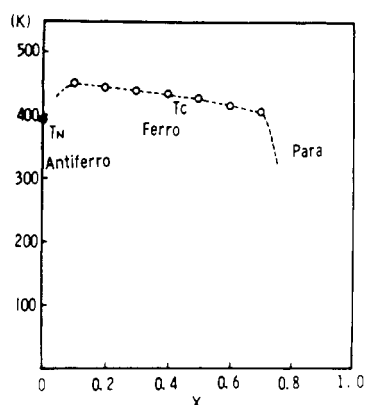
The ferromagnetic moments per molecule calculated from the value of the saturation magnetization extrapolated to 0 K are shown in Figure 7. According to this figure, the Cr and Mo atoms may likely play the same role in the magnetic properties of both solid solutions. The ferromagnetic moment

(7) Goodenough, J. B. "Magnetism and the Chemical Bond"; Interscience: New York, 1963; p 115.

Table I. Structure Factors of $(\text{Mn}_{1-x}\text{Mo}_x)_3\text{B}_4$ ^a

hkl	Mn_3B_4		$(\text{Mn}_{0.6}\text{Mo}_{0.4})_3\text{B}_4$				$(\text{Mn}_{0.5}\text{Mo}_{0.5})_3\text{B}_4$				$(\text{Mn}_{0.3}\text{Mo}_{0.7})_3\text{B}_4$			
	obsd	calcd	obsd	calcd (1)	calcd (2)	calcd (3)	obsd	calcd (1)	calcd (2)	calcd (3)	obsd	calcd (1)	calcd (2)	calcd (3)
(110)	54	51	65	51	64	59	62	50	63	57	77	50	61	67
(031)	92	93	97	96	96	90	96	96	96	98	96	98	98	91
(060)	103	83	88	83	87	84	83	83	87	86	82	84	87	86
(150)	100	100	100	100	100	100	100	100	100	100	100	100	100	100
(121)	84	87	90	92	90	92	87	85	90	87	86	84	88	91
(141)	35	42	40	36	53	38	35	34	51	40	34	31	45	56
(071)	43	58	44	53	65	65	37	53	64	56	38	50	60	67

^a Key: calcd(1), Mo atoms have preference for the 4(g) site; calcd(2), Mo atoms have preference for the 2(c) site; calcd(3), Mo atoms have random occupancy.

Figure 8. Magnetic phase diagram of $(\text{Mn}_{1-x}\text{Cr}_x)_3\text{B}_4$.

did not change in the range of $0.1 \leq x \leq 0.3$ but decreased rapidly for $x \geq 0.4$. This result is probably related to the site preference of Cr and Mo atoms for the 4(g) site of the Ta_3B_4 structure. The chromium and molybdenum atoms without magnetic moments predominantly occupy the 4(g) site in the compositional range $0.1 \leq x \leq 0.3$, but in the range of $x \geq 0.4$ they are distributed randomly between 4(g) and 2(c) sites of the Ta_3B_4 structure.

For the clarification of the site preference of Cr and Mo atoms for the 4(g) site of Ta_3B_4 structure, the distribution of Mo atoms was examined by the intensity measurement of X-ray powder patterns for $(\text{Mn}_{0.6}\text{Mo}_{0.4})_3\text{B}_4$, $(\text{Mn}_{0.5}\text{Mo}_{0.5})_3\text{B}_4$, and $(\text{Mn}_{0.3}\text{Mo}_{0.7})_3\text{B}_4$. Both observed and calculated intensities are listed in Table I. Considering the fact that the number of available Mn4(g) sites is twice that of the 2(c) site, it can be said that Mo atoms have site preference at the 4(g) site statistically.

The magnetic phase diagrams of $(\text{Mn}_{1-x}\text{Cr}_x)_3\text{B}_4$ and $(\text{Mn}_{1-x}\text{Mo}_x)_3\text{B}_4$ are illustrated in Figures 8 and 9. As shown in Figure 8, the Curie temperature decreases slightly from 450 to 400 K with increasing Cr content and above $x = 0.8$ its magnetic properties are paramagnetic down to 4.2 K. On the other hand, the compositional dependence of Curie temperature in the system $(\text{Mn}_{1-x}\text{Mo}_x)_3\text{B}_4$ was quite different from that of $(\text{Mn}_{1-x}\text{Cr}_x)_3\text{B}_4$. In the $(\text{Mn}_{1-x}\text{Mo}_x)_3\text{B}_4$ system, the Curie temperature increases from 400 to 550 K with a maximum value of 550 K at $x = 0.3$.

It is generally thought that, in alloys or intermetallic compounds containing Mn atoms, the magnetic interaction is closely related to the nearest Mn-Mn distance. Guillaud⁸ and Forrer⁹ experimentally determined a critical distance of 0.28 nm separating the ferromagnetic and antiferromagnetic coupling regimes. This relationship is shown in Figure 10 for several compounds.

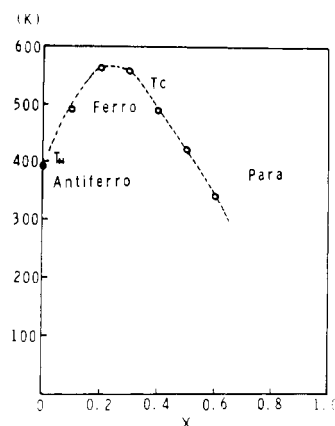
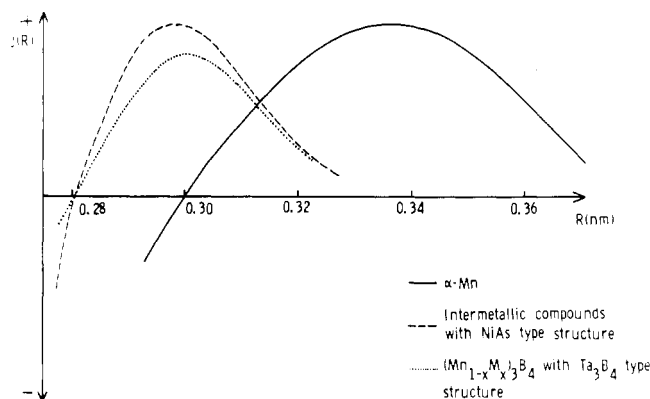
Figure 9. Magnetic phase diagram of $(\text{Mn}_{1-x}\text{Mo}_x)_3\text{B}_4$.

Figure 10. Relationship between magnetic interaction and nearest Mn-Mn distance. R (nm) is the nearest Mn-Mn distance and $J(R)$ is the exchange energy that is estimated from the Curie temperature. The dashed curve was obtained by Samara,¹⁰ and the dotted curve is our present work.

Samara¹⁰ proposed that in the intermetallic compounds with the NiAs type structure, as shown in Figure 10, the curve exhibited a maximum at about $R = 0.30$ nm, where R is the nearest Mn-Mn distance. Yamada deduced the proposed relation between magnetic interaction and the nearest Mn-Mn distance for α -Mn from the results of the magnetic structure.¹¹

Considering the model proposed by Guillaud and by Samara mentioned above, the difference in compositional dependence of the Curie temperature for both solid solutions could be well explained as follows. Since the nearest Mn-Mn distance, which is equal to the c axis in the present systems, decreases slightly in $(\text{Mn}_{1-x}\text{Cr}_x)_3\text{B}_4$, the Curie temperature decreases slightly with increasing x . On the other hand, in the system

(8) Guillaud, C. *Rev. Mod. Phys.* **1952**, *25*, 121.(9) Forrer, R., *Ann. Phys. (Paris)* **1952**, *7*, 605.(10) Samara, G. A.; Giardini, A. A. *Phys. Solids High Pressures, Proc. Int. Conf., 1st 1965*, 309.(11) Yamada, T.; Kunitomi, N. *J. Phys. Soc. Jpn.* **1970**, *28*, 615.

(Mn_{1-x}Mo_x)₃B₄ the *c* axis changes from 0.295 to 0.305 nm, and it is expected that the nearest Mn-Mn distance crosses the maximum point of the exchange energy and the Curie temperature shows the indicated cuplike variation. It seems that the relation between magnetic interaction and nearest Mn-Mn distance is quite similar to that of NiAs type intermetallic compounds.

Registry No. Mn₃B₄, 12229-02-6; Cr₃B₄, 12045-71-5; Mo₃B₄, 12310-46-2.

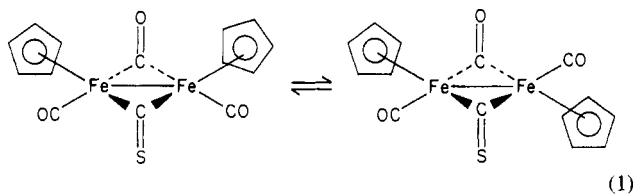
Contribution from the Department of Chemistry,
Iowa State University, Ames, Iowa 50011

Lewis Acid Adducts of the Bridging Thiocarbonyl in (η -C₅H₅)₂Fe₂(CO)₃(CS)

Michael H. Quick¹ and Robert J. Angelici*

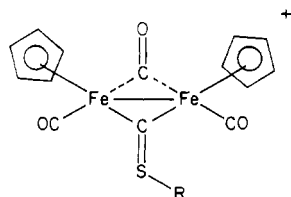
Received September 22, 1981

We recently described the synthesis of the thiocarbonyl-bridged Cp₂Fe₂(CO)₃(CS) dimer (Cp = η -C₅H₅).^{2,3} Like the ruthenium analogue,⁴ Cp₂Ru₂(CO)₃(CS), the iron dimer exists in solution as an equilibrium mixture of the cis and trans isomers:



An X-ray diffraction study has established the structure of the cis isomer in the solid state.⁵

The reactivity of Cp₂Fe₂(CO)₃(CS) has a certain similarity to that of Cp₂Fe₂(CO)₄. It reacts with phosphines, phosphites, and CNMe to give the substituted Cp₂Fe₂(CO)₂(L)(CS) products.⁶ It is cleaved by Na amalgam, yielding CpFe(CO)(CS)⁻ and CpFe(CO)₂⁻². On the other hand, its reactivity² with Me₂S₂, halogens, and O₂ with HBF₄ is quite different than is observed with Cp₂Fe₂(CO)₄. Also Cp₂Fe₂(CO)₃(CS) reacts readily with alkyl iodides and other alkylating agents to give the S-alkylated products:^{3,6}



While no CO-alkylated products of Cp₂Fe₂(CO)₄ have been reported, certain Lewis acids such as AlEt₃ do form adducts

with the bridging CO groups.⁷⁻⁹ In the present report, we describe Lewis acid adducts of the bridging CS group in Cp₂Fe₂(CO)₃(CS). Related to this research is the report of the formation of Lewis acid adducts of the triply bridging CS in (CpCo)₃(S)(CS).¹⁰ Also, it is well-known that terminal CS groups in electron-rich complexes form adducts with Lewis acids and are alkylated at the CS sulfur atom.¹¹⁻¹⁴

Experimental Section

General Procedures. All reactions were carried out under a pre-purified N₂ atmosphere with use of Schlenk equipment. Unless indicated otherwise, reactions were conducted at room temperature.

Molar conductivities were measured in nitromethane solutions at 25 °C with an Industrial Instruments RC-16B2 conductivity bridge. A Perkin-Elmer 337 or 237B instrument was used to record infrared spectra; 1-mm path length NaCl cells were used for most spectra, which were calibrated with CO gas (CO region) and polystyrene (CS region); band positions are believed to be accurate to within ±2 cm⁻¹. Proton NMR spectra were recorded on a Varian HA-100 spectrometer, with tetramethylsilane (Me₄Si) as an internal reference. Elemental analyses were performed by Galbraith Laboratories.

Solvents and Reagents. Nitromethane for conductivity measurements was dried over P₄O₁₀, fractionally distilled twice under N₂, and stored over type 4A molecular sieves under N₂. All other solvents were reagent grade and were stored over 4A sieves and purged with N₂ before use.

The thiocarbonyl complex Cp₂Fe₂(CO)₃(CS) was prepared as previously described.² The carbonyl complexes Et₄N[M(CO)₅I] (M = Cr, W)¹⁵ and [CpFe(CO)₂(THF)]BF₄¹⁶ were prepared by literature methods. All other reagents were of the highest purity available and were used as received.

Cp₂Fe₂(CO)₃CS·HgX₂ (X = Cl, Br, I). Mercuric iodide (0.227 g, 0.500 mmol) was added to a solution of Cp₂Fe₂(CO)₃(CS) (0.187 g, 0.505 mmol) in 30 mL of acetone, and the mixture was stirred for 10 min. Evaporation of the solvent under reduced pressure gave a dark red residue, which was dried in vacuo for several hours. The product was transferred to a frit filter, washed thoroughly 10 times with 20 mL of pentane, and again vacuum-dried. Yield of the product, Cp₂Fe₂(CO)₃CS·HgI₂, was essentially quantitative. Anal. Calcd for C₁₄H₁₀Fe₂HgI₂O₃S: C, 20.40; H, 1.22. Found: C, 19.87; H, 1.34.

The adducts Cp₂Fe₂(CO)₃CS·HgCl₂ and Cp₂Fe₂(CO)₃CS·HgBr₂ were obtained in the same manner, except that CH₂Cl₂ was used as the solvent.

[Cp₂Fe₂(CO)₃CS·HgMe]PF₆. Methylmercuric chloride (0.13 g, 0.52 mmol) was dissolved in 15 mL of CH₂Cl₂ at 0 °C, and AgPF₆ (0.13 g, 0.51 mmol) in 10 mL of CH₂Cl₂ was added. The mixture was stirred for 15 min and then Cp₂Fe₂(CO)₃(CS) (0.20 g, 0.54 mmol) was added, giving a dark red mixture. After 5 min the solution was filtered to remove AgCl, 30 mL of hexane was added, and the solution was evaporated; the crystals thus obtained were filtered off and washed with Et₂O. Two more crystallizations in this manner gave dark red needles of [Cp₂Fe₂(CO)₃CS·HgMe]PF₆ sufficiently pure for analysis (0.25 g, 67%). Anal. Calcd for C₁₅H₁₃Fe₂HgO₃PS: C, 24.66; H, 1.79. Found: C, 24.99; H, 1.86.

Cp₂Fe₂(CO)₃CS·M(CO)₅ (M = Cr, W). A solution of Et₄N[Cr(CO)₅I] (0.229 g, 0.510 mmol) in 30 mL of acetone was cooled to 0 °C, and then AgBF₄ (0.100 g, 0.513 mmol) in 10 mL of acetone was added over 5 min from an equippressure dropping funnel. After an additional 10 min, the mixture was filtered under N₂ to remove AgI, and the yellow-orange filtrate was again cooled to 0 °C. The thiocarbonyl complex (0.191 g, 0.516 mmol) was added, and the

- (1) Based on the Ph.D. dissertation submitted by M.H.Q. to Iowa State University, 1978.
- (2) Quick, M. H.; Angelici, R. J. *J. Organomet. Chem.* **1978**, *160*, 231.
- (3) Wagner, R. E.; Jacobson, R. A.; Angelici, R. J.; Quick, M. H. *J. Organomet. Chem.* **1978**, *148*, C35.
- (4) Wnuk, T. A.; Angelici, R. J. *Inorg. Chem.* **1977**, *16*, 1173.
- (5) Beckman, D. E.; Jacobson, R. A. *J. Organomet. Chem.* **1979**, *179*, 187.
- (6) Quick, M. H.; Angelici, R. J. *Inorg. Chem.* **1981**, *20*, 1123.

- (7) Alich, A.; Nelson, N. J.; Strobe, D.; Shriver, D. F. *Inorg. Chem.* **1972**, *11*, 2976.
- (8) Kim, N. E.; Nelson, N. J.; Shriver, D. F. *Inorg. Chim. Acta* **1973**, *7*, 393.
- (9) Shriver, D. F. *J. Organomet. Chem.* **1975**, *94*, 259.
- (10) Werner, H.; Leonhard, K.; Kolb, O.; Röttinger, E.; Vahrenkamp, H. *Chem. Ber.* **1980**, *113*, 1654.
- (11) Dombek, B. D.; Angelici, R. J. *J. Am. Chem. Soc.* **1974**, *96*, 7568.
- (12) Dombek, B. D.; Angelici, R. J. *J. Am. Chem. Soc.* **1975**, *97*, 1261.
- (13) Dombek, B. D.; Angelici, R. J. *Inorg. Chem.* **1976**, *15*, 2397.
- (14) Greaves, W. W.; Angelici, R. J. *J. Organomet. Chem.* **1980**, *191*, 49.
- (15) Greaves, W. W.; Angelici, R. J. *Inorg. Chem.* **1981**, *20*, 4108.
- (16) Abel, E. W.; Butler, I. S.; Reid, J. G. *J. Chem. Soc.* **1963**, 2068.
- (17) Reger, D. L.; Coleman, C. J. *J. Organomet. Chem.* **1977**, *131*, 153.